

Conjugate natural-convection–conduction heat transfer in enclosures divided by horizontal fins

C. J. Ho and J. Y. Chang

Department of Mechanical Engineering, National Cheng Kung University, Tainan, Taiwan, Republic of China

This article presents a numerical study concerning conjugate heat transfer across a vertical rectangular water-filled enclosure divided by multiple horizontal fins. The objective of the study is mainly to explore the effects of the conducting horizontal fins on heat transfer due to conjugate natural convection–conduction in the finned enclosure. Numerical results via a finite-difference method for the governing differential equations of the problem considered have been obtained for two different conductive fins with $Ra = 10^3$ to 10^7 , $AR = 1, 5, 8,$ and 10 , $N = 1$ to 4 , and $t = 0.00001$ to 0.125 . The results demonstrate that the feasibility and effectiveness of using horizontal fins to enhance heat transfer across a vertical rectangular enclosure depend strongly on the aspect ratio, the Rayleigh number, the thermal conductivity, and the number of fins in the enclosure.

Keywords: conjugate natural convection; partitioned enclosure

Introduction

Natural convection in enclosures is an important electronic-equipment cooling technique due to its inherent reliability, simplicity, and absence of noise. One way to increase the overall heat transfer from the heat-dissipating surface in an enclosure is to apply localized-conduction cooling fins to connect the hot and cold surfaces, as in the configuration considered in this study (illustrated schematically in Figure 1). Heat is dissipated from the hot wall to the cold wall of the enclosure by the conjugate convection of fluid in the divided subenclosures and conduction in the horizontal fins.

Although the literature on natural convection in differentially heated enclosures is voluminous, as revealed in the recent comprehensive review by Ostrach (1988), until recently considerable interest has been given to the problem of natural convection in partially or fully divided enclosures, due to its fundamental importance in connection with complex natural-convection phenomena arising in various technological applications. Typical examples include thermal insulation, solar-collector design, reactor thermal hydraulics, and fire protection, to name a few. Some of the representative works in this area are those of Nansteel and Greif (1981), Bajorek and Lloyd (1982), Lin and Bejan (1983), Acharya and Tsang (1985), Tong and Gerner (1986), Ho and Yih (1987), Mishimura et al. (1988), Ho and Jeng (1989), Acharya and Jetli (1990), Oosthuizen and Paul (1985), Shakerin et al. (1986), Frederick (1989), and Kangni et al. (1991). A comprehensive review of this subject is available in the paper of Acharya and Jetli (1990). These early works have shown that natural-convection heat

transfer in a vertical enclosure with a partial or full vertical partition fitted to its adiabatic walls can be considerably reduced in comparison with that for a nondivided enclosure at the same Rayleigh number. The reduction in heat transfer is found to be further induced with an increasing number of vertical partitions.

Unlike the heat transfer problem in an enclosure fitted with vertical partitions, the effects of a horizontal fin attached to thermally active walls of an enclosure were fragmentary. Oosthuizen and Paul (1985) numerically analyzed natural convection in an air-filled vertical cavity with a horizontal plate on the cold wall, and an increase in heat transfer was found for the adiabatic or perfectly conducting plate. Also, a slight heat transfer augmentation was reported for a discrete rough element on the vertical heated wall of an enclosure (Shakerin et al. 1986). In contrast, a heat transfer reduction due to a diathermal partial partition on the cold wall of an air-filled, inclined square cavity was found by Frederick (1989). It is apparent from these early studies that the effects of the horizontal fin (partition) on the natural-convection heat transfer in an enclosure remain unclear, and there is a need for further study in the area.

Mathematical formulation

As depicted in Figure 1, two-dimensional (2-D) steady conjugate natural-convection-conduction heat transfer in a vertical rectangular enclosure divided by horizontal fins is considered. The enclosure is fully divided into equal sub-enclosures by the horizontal fins of finite thickness, t^* , and thermal conductivity, k_s . The vertical endwalls of the enclosure are maintained isothermal at different temperatures, T_h and T_c , respectively, while the horizontal endwalls are assumed to be adiabatic. The buoyancy-driven flow in the subenclosures is assumed to be laminar. The thermophysical properties of the

Address reprint requests to Professor Ho at the Department of Mechanical Engineering, National Cheng Kung University, Tainan, Taiwan, Republic of China.

Received 25 February 1992; accepted 7 July 1992

© 1993 Butterworth-Heinemann

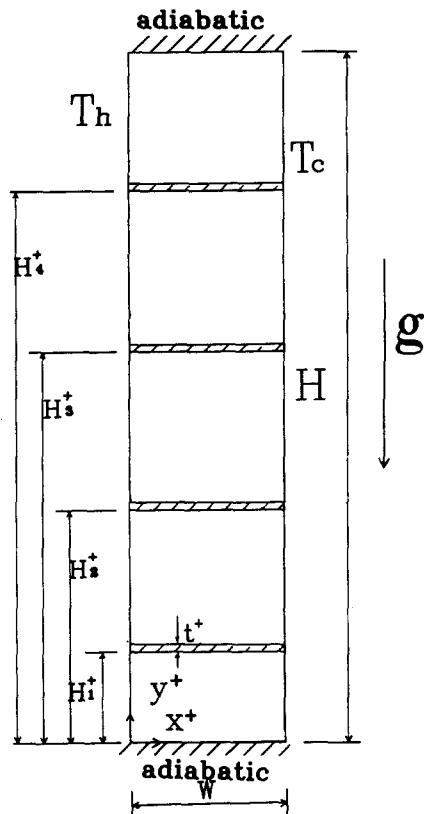


Figure 1 Schematic description of the physical configuration

fluid except density are assumed to be temperature independent, adhering to the Oberbeck-Boussinesq approximation. Further, the viscous dissipation and compressibility effects are neglected. In the horizontal solid fins, 2-D conduction heat transfer is considered.

The dimensionless governing partial differential equations under the foregoing assumptions for the conjugate heat transfer

problem considered can be written in terms of vorticity, stream function, and temperature as follows.

In the fluid-filled subenclosures,

$$\frac{\partial \psi}{\partial y} \frac{\partial \omega}{\partial x} - \frac{\partial \psi}{\partial x} \frac{\partial \omega}{\partial y} = \text{Pr} \left(\frac{\partial^2 \omega}{\partial x^2} + \frac{\partial^2 \omega}{\partial y^2} \right) + \text{PrRa} \frac{\partial \theta}{\partial x} \quad (1)$$

$$\frac{\partial^2 \psi}{\partial x^2} + \frac{\partial^2 \psi}{\partial y^2} = -\omega \quad (2)$$

$$\frac{\partial \psi}{\partial y} \frac{\partial \theta}{\partial x} - \frac{\partial \psi}{\partial x} \frac{\partial \theta}{\partial y} = \frac{\partial^2 \theta}{\partial x^2} + \frac{\partial^2 \theta}{\partial y^2} \quad (3)$$

In the solid fins,

$$\frac{\partial^2 \theta}{\partial x^2} + \frac{\partial^2 \theta}{\partial y^2} = 0 \quad (4)$$

The boundary conditions for this problem are

$$x = 0; \psi = 0, \theta = 1 \quad (5a)$$

$$x = 1; \psi = 0, \theta = 0 \quad (5b)$$

$$y = 0 \text{ or } \text{AR}; \psi = 0, \frac{\partial \theta}{\partial y} = 0 \quad (5c)$$

Moreover, the continuity of the temperature field and conservation of energy at the surfaces of the horizontal fins exposed to the fluid require

$$(\theta)_f = (\theta)_s; \left(\frac{\partial \theta}{\partial y} \right)_f = \text{KR} \left(\frac{\partial \theta}{\partial y} \right)_s \quad (5d)$$

The average heat transfer coefficient on the fluid-wetted vertical surfaces of the enclosure is presented as an average Nusselt number of the form

$$(\overline{\text{Nu}})_N = \frac{\bar{q}_f}{k_f(T_h - T_c)} \quad (6)$$

where \bar{q}_f is the average heat flux at the fluid-wetted hot wall of the finned enclosure and the subscript N denotes the number of fins fitted in the enclosure. Moreover, the total heat

Notation

AR	Aspect ratio, H/W
g	Gravitational acceleration
h	Heat transfer coefficient
H	Height of enclosure
H_i^+	Locations of fins
H_i	Dimensionless locations of fins, H_i^+/W
k	Thermal conductivity
KR	Thermal conductivity ratio, k_s/k_f
N	Number of fins
Nu	Nusselt number
Pr	Prandtl number
q	Heat flux
Ra	Rayleigh number, $g\beta(T_h - T_c)W^3/(v\alpha)$
t^+	Thickness of fin
t	Dimensionless thickness of fin, t^+/W
T	Temperature
W	Width of enclosure
x^+, y^+	Cartesian coordinates
x, y	Dimensionless coordinates, $x^+/W, y^+/W$

Greek symbols

α	Thermal diffusivity
β	Thermal expansion coefficient
ε	Heat transfer effectiveness of finned enclosure
θ	Dimensionless temperature, $(T - T_c)/(T_h - T_c)$
Θ	Dimensionless heat function
ν	Kinematic viscosity
ψ^+	Stream function
ψ	Dimensionless stream function, ψ^+/α
ω^+	vorticity
ω	Dimensionless vorticity, ω^+W^2/α

Subscripts

c	Cold wall
f	Fluid
h	Hot wall
i	The i th subenclosure
N	Enclosure divided by N fins
s	Solid fin
t	Total

Superscript

—	Surface averaged value
---	------------------------

transfer rate across the finned enclosure, including the conduction through the fins and natural convection in the subenclosures, is expressed by a dimensionless total heat flux:

$$(\bar{q}_t)_N = \frac{1}{AR} \left\{ \int_0^{H_1} - \left(\frac{\partial \theta}{\partial x} \right)_{x=0} dy + \sum_{i=1}^N \left[\int_{H_i}^{H_{i+1}} - \left(\frac{\partial \theta}{\partial x} \right)_{x=0} dy + \int_{H_{i+1}}^{H_{i+2}} - \left(\frac{\partial \theta}{\partial x} \right)_{x=0} dy \right] \right\} \quad (7)$$

Numerical method

The system of governing differential equations (Equations 1 to 4) together with the boundary conditions (Equations 5a to 5d) is solved by means of a finite-difference method. A fourth-order central-difference formula was used for the diffusion terms in the differential equations, while the 2-D QUICK scheme (Leonard 1983) was adopted for the convective terms. The resulting system of finite-difference equations was solved iteratively via a line-by-line relaxation scheme; the pentadiagonal coefficient matrix of the system of algebraic equations due to the higher-order finite-difference scheme used here was effectively treated by incorporating the PDMA (PentaDiagonal Matrix Algorithm) (Fletcher 1988). The steady-state solutions to the problem under consideration were obtained with a prescribed relative convergence criterion of 10^{-5} for each field variable of the problem. The converged solutions were further examined for the energy balance across the vertical walls of the enclosure at least within 1 percent.

The numerical calculations were conducted over a mesh system consisting of a piecewise uniform grid size in the vertical



Figure 2 Typical grid system of 41 x 241 for AR = 10

Table 1 Typical convergence of Nusselt number in a water-filled partitioned enclosure with grid size, KR = 1, $t = 0.005$, and $Ra = 10^6$

AR	N	Mesh	\bar{Nu}	Mesh	\bar{Nu}
1	2	31 x 39 (5)*	6.644	31 x 69 (5)	6.862
		31 x 99 (5)	6.899	31 x 77 (9)	6.870
10	2	31 x 99 (5)	6.132	31 x 129 (5)	6.420
		31 x 158 (5)	6.450		
10	4	41 x 151 (11)	6.492	41 x 201 (11)	7.151
		41 x 241 (11)	7.268	41 x 281 (11)	7.309

* The number in parentheses is the vertical grid points laid across each fin thickness.

(y) direction and a nonuniform grid space in the horizontal (x) direction, as exemplified in Figure 2 for AR = 10. The nonuniform grids in the x direction were distributed systematically so as to have denser grids adjacent to both vertical walls of the enclosure. Moreover, a series of tests for convergence of the calculations with the grid size was performed using various mesh systems as exemplified in Table 1 for KR = 1, $t = 0.005$, $Ra = 10^6$, AR = 1 and 10, N = 2 and 4; several mesh systems ranging from 31 x 61 to 41 x 241 were used for the calculations, mainly depending on the aspect ratio, the number of fins, and the Rayleigh number. Of the piecewise uniform vertical grid lines, 11 to 21, depending on the number of fins, were laid across each horizontal fin.

Moreover, the computer code developed in the present study was validated for a fully air-filled enclosure with an aspect ratio of both one and ten. Tables 2 and 3 show, respectively, the comparisons of the heat transfer results as well as the stream function extreme with the benchmark results for the square enclosure (de Vahl Davis 1983; Saitoh and Hirose 1989) and with the average Nusselt number data for the tall enclosure of AR = 10 (Ramman and Korpela 1989). It is clear that the present predictions were in good agreement with the data in the literature.

Results and discussion

From the mathematical formulation of the problem under consideration, it is evident that the flow field and temperature distribution in the finned enclosure are governed by the following dimensionless parameters: the Prandtl number (Pr), the Rayleigh number (Ra), the thermal conductivity ratio (KR), the aspect ratio (AR), the number of fins (N), and the dimensionless thickness of the fin (t). In the present study, parametric calculations have been conducted to explore primarily the effects of the horizontal dividing fins on the conjugate heat transfer and fluid flow across the finned enclosure. The fluid filling the divided subenclosures that are considered here is water (Pr = 6.5), with the other parameters in the following ranges: $Ra = 10^3$ to 10^7 ; KR = 1 and 390 (aluminum fins); AR = 1, 5, 8, and 10; N = 1 to 4; and $t = 0.00001$ to 0.125.

Heat and fluid flow fields

First of all, the heat and fluid flow fields developed in the finned enclosure are presented by means of contour plots of isotherms (or heatlines) and streamlines, respectively. Here the heatlines are based on the concept of heat function developed by Bejan (1984). In the presence of multiple horizontal fins, as demonstrated by the streamline and isotherm plots shown in

Table 2 Comparison of Nusselt number and stream function with the benchmark solutions for an air-filled square enclosure

Ra	$(\bar{Nu}, \psi_{mid}, \psi_{max})$		
	de Vahl Davis (1983)	Saitoh and Hirose (1989)	Present study
10^4	(2.238, 5.102, 5.102)	(2.241, —, —)	(2.249, 5.143, 5.143)
10^5	(4.509, —, —)	—	(4.510, —, —)
10^6	(8.817, 16.32, 16.75)	(8.484, —, —)	(8.771, 16.57, 17.07)

Table 3 Average Nusselt number for an air-filled tall enclosure, AR = 10

Ra	\bar{Nu}	
	Ramman and Korpela (1989)	Present study
1.42×10^4	1.884	1.880
5.68×10^4	2.811	2.747
7.1×10^4	2.975	2.825

Figures 3 and 4 for AR = 1 and 10, respectively, the diagonal symmetry of the flow structure and the temperature distribution in the finned enclosure appear to be preserved as in the case of the fully fluid-filled vertical rectangular enclosure.

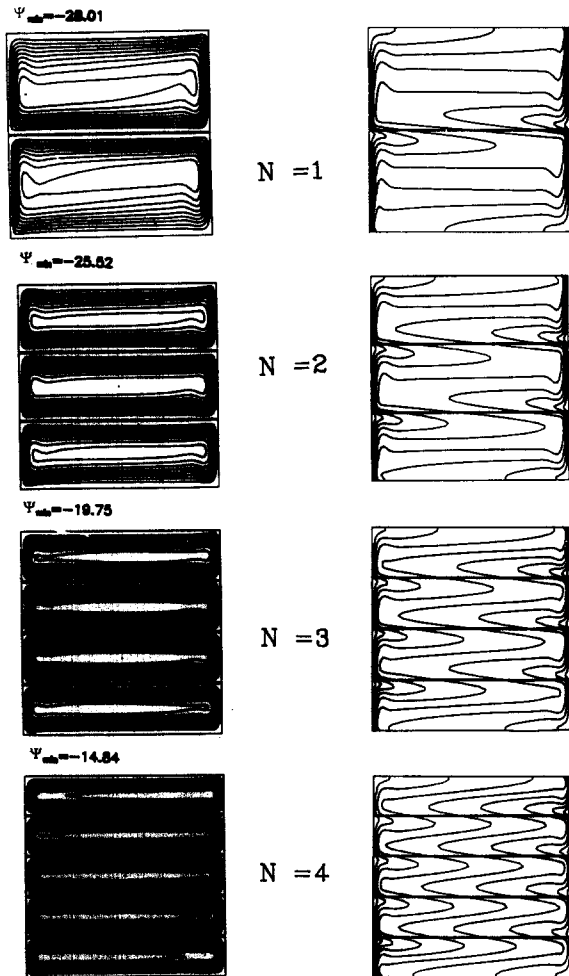


Figure 3 Flow structure (left) and temperature distribution (right) for $Ra = 10^7$ in a square enclosure with various numbers of dividing horizontal fins of $t = 0.005$ and $KR = 1$

Further inspection of the figures reveals that an increase in the number of fins in an enclosure with fixed aspect ratio results in weaker fluid flow in the subenclosures, as indicated by the decreasing minimum values of the stream function. For temperature distribution, as shown by the isotherms in Figures 3 and 4, the development of the thermal boundary layer along the vertical walls of the enclosure is interrupted by the presence of the solid fins and redevelops across the downstream subenclosure. This is the mechanism that may result in heat-dissipation enhancement from the fluid-wetted hot wall.

Figures 5 and 6 exemplify the influence of Ra on the patterns of streamlines (left), isotherms (middle), and heatlines (right) in the enclosure with aspect ratio of 1 and 10, respectively, with four horizontal fins of $KR = 1$. For the square enclosure (Figure 5) at $Ra = 10^3$, the heat transfer across the finned enclosure is expected to be conduction dominated, as demonstrated by the evenly spaced vertical isotherms as well as the nearly straight heatlines emanating from the hot vertical wall toward the cold wall of the enclosure. Further, the isotherms as well as the heatlines at $Ra = 10^5$ display pseudoconduction characteristics; heat from the fluid-wetted hot wall in each subenclosure is mainly channeled through a horizontal corridor near the ceiling of the subenclosure, as indicated by the deformed heatlines there. Closer examination of the heatlines reveals that some of the heatlines emanating from the fluid-wetted hot wall of the lower subenclosure pass across the dividing fin entering and terminating at the adjacent subenclosure above. This clearly demonstrates the heat transfer

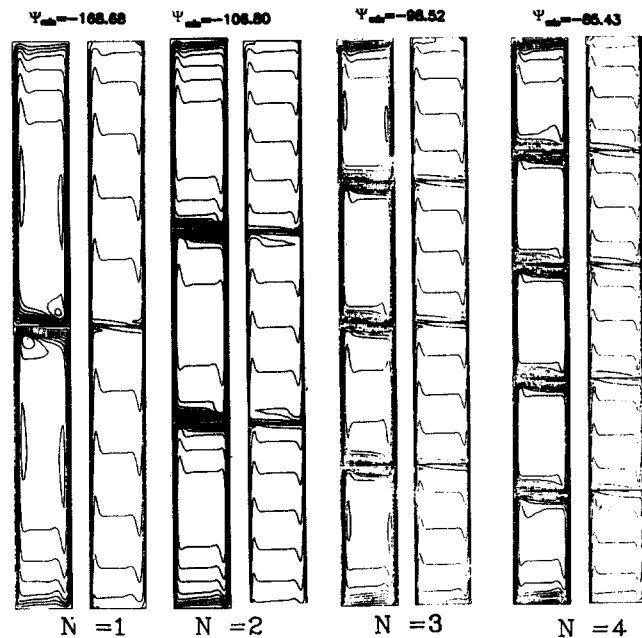


Figure 4 Flow structure (left) and temperature distribution (right) for $Ra = 10^7$ in a tall enclosure of AR = 10 with various numbers of fins of $t = 0.005$ and $KR = 1$

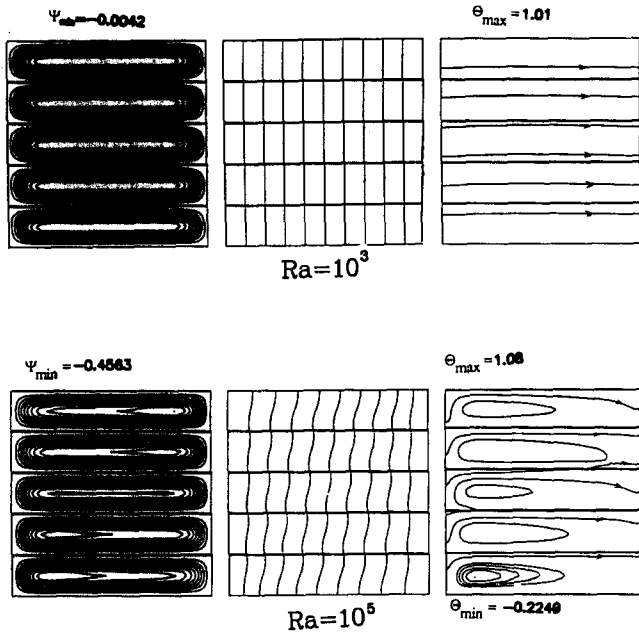


Figure 5 Contours of streamlines (left), isotherms (middle), and heatlines (right) in a square finned enclosure with $N = 4$, $t = 0.005$, and $KR = 1$

interaction between the adjoining subenclosures through the conducting fins. For the tall vertical enclosure, as shown in Figure 6 for $AR = 10$, the effects of increasing Ra on the heat and fluid flow structure become further pronounced.

Next, Figure 7 presents the heat and fluid flow structure in a square finned enclosure with $KR = 390$. Complemented by

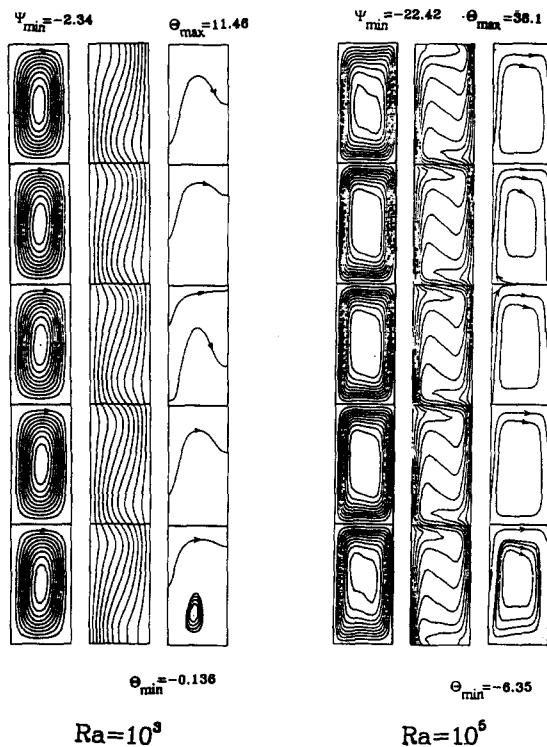


Figure 6 Contours of streamline (left), isotherms (middle), and heatlines (right) in a tall enclosure of $AR = 10$ with $N = 4$, $t = 0.005$, and $KR = 1$

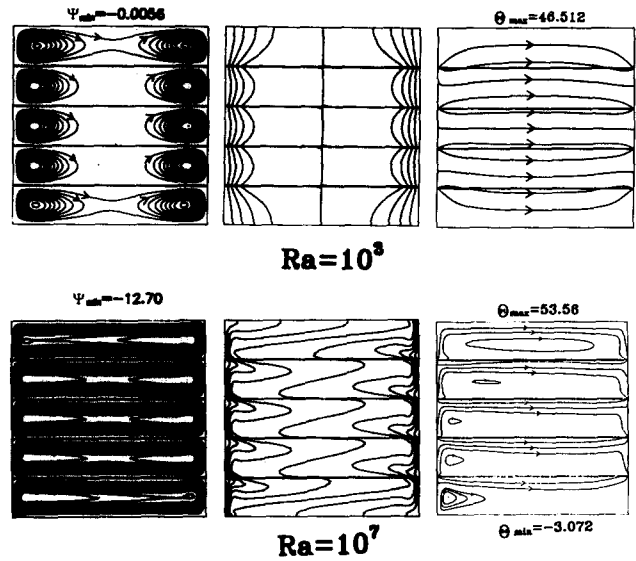


Figure 7 Fluid and heat flow patterns in a square enclosure fitted with four aluminum fins ($KR = 390$)

Figures 3 and 5, Figure 7 is intended to illustrate the effect of the thermal conductivity ratio. The fluid flow in the enclosure divided by the highly conductive fins, in comparison with Figures 3 and 5 for $KR = 1$, appears to be markedly affected, as indicated by the different magnitude of the minimum stream function shown in Figure 7. For the lower Rayleigh number, $Ra = 10^3$, heat transfer across the finned enclosure with $KR = 390$, as indicated by the deformation of the isotherms as well as of the heatlines in Figure 7, can be seen to be greatly enhanced due to the presence of the highly conductive fins in the square enclosure. At a higher Rayleigh number, 10^7 , the isotherms in Figure 7 clearly indicate that the highly conductive fins induce a thinner thermal boundary layer than that observed in Figure 3 for $KR = 1$ at the same Ra .

In Figure 8, the influence of the fin thickness on the flow field and the temperature distribution is displayed for a tall finned enclosure with three values of t with $N = 4$, $KR = 390$, and $Ra = 10^6$. As is generally expected, the increase of the fin thickness tends to induce moderately weaker flow strength in the subenclosures as a result of its decreasing aspect ratio, as indicated by the decreasing magnitude of the minimum stream function with increasing t shown in Figure 8. Moreover, the isotherms in Figure 8 reveal that with the fin thickness greater than 0.025, the dividing fins of $KR = 390$ tend to behave like a perfectly conducting endwall for each subenclosure, as demonstrated by the evenly spaced isotherm across the fins.

Heat transfer results

Now the results of the heat transfer rate across the finned enclosure will be considered. In order to elucidate the effect of the horizontal fins on the heat transfer rate across the enclosure, additional calculations have been performed in the present study for the case of a fully-filled enclosure ($N = 0$). Figure 9 conveys the typical results of the average Nusselt number on the fluid-wetted vertical hot wall \bar{Nu} in a square enclosure at various Rayleigh numbers. For $KR = 1$ with $t = 0.005$, it is clear from the figure that the average Nusselt number for the finned square enclosure, in comparison to the enclosure without fins ($N = 0$), is markedly reduced as the number of fins is increased; however, the reduction in \bar{Nu} tends to diminish with increasing Rayleigh number. As for the highly conductive

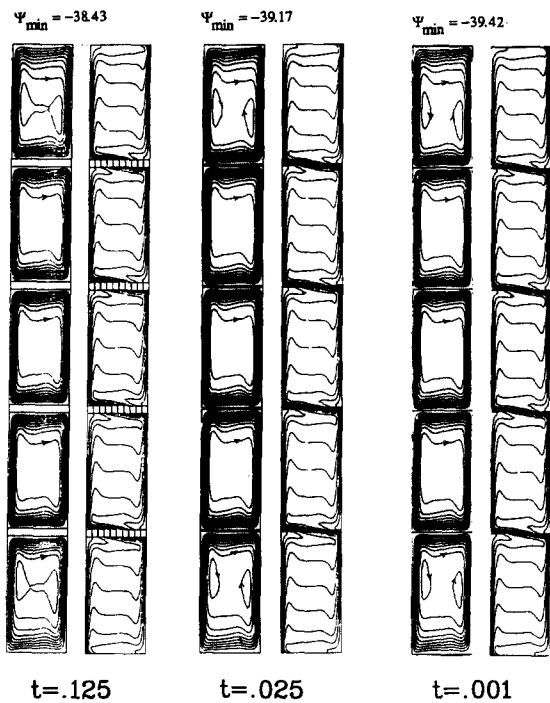


Figure 8 Fluid and heat flow structure in a tall enclosure (AR = 10) with four aluminum fins of various thickness at Ra = 10⁶

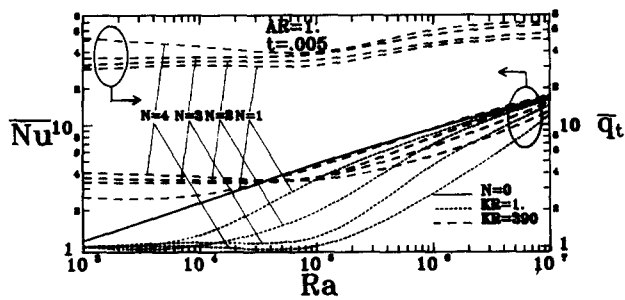


Figure 9 Relation of average Nusselt number and total heat flux across a square enclosure with Rayleigh number

fin, KR = 390, the foregoing reduction in \bar{Nu} due to the dividing fin occurs only with the Rayleigh number approximately greater than 4×10^4 ; below that, a significant increase in \bar{Nu} due to the presence of the fins can be readily detected, as shown in Figure 9. To further quantify the fin effect, a modified average Nusselt number \bar{Nu}^* is defined as

$$\bar{Nu}^* = \frac{(\bar{Nu})_N}{(\bar{Nu})_{N=0}} \quad (8)$$

and is plotted versus the Rayleigh number in Figure 10. It can be noticed that with aluminum fins (KR = 390) and low Rayleigh number (10^3), the conduction-dominated heat transfer from the fluid-wetted hot wall of a square enclosure can be drastically enhanced with increasing number of fins, indicative of a significant contribution of conduction through the highly conductive fins. With increasing Rayleigh number, the modified average Nusselt number curves for KR = 390 shows a significant decline reaching a minimum at a certain Ra and thereafter give way to a flat increasing trend. Another important fact that can be observed in Figure 10 is that the modified average Nusselt number for the finned square enclosure with KR = 390 is always greater than that with

KR = 1; however, the disparity is greatly decreased with the increasing Rayleigh number.

Also shown in Figure 9 is the total heat flux across the finned square enclosure, which is another important heat transfer quantity of the problem under consideration. It should be noted that the values of \bar{q}_t for KR = 1 in Figure 9 are approximately equal to those of \bar{Nu} , due to the low thermal conductivity and small fin thickness. The total heat flux across the finned square enclosure appears to be a strong function of the thermal conductivity of the fins, the number of fins, and the Rayleigh number. For KR = 1, the presence of dividing fins tends to result in a reduction in total heat transfer rate; but with aluminum fins, the total heat flux is found to be considerably enhanced with increasing number of fins, as indicated in Figure 9. Moreover, the total heat transfer performance of the finned enclosure is assessed by plotting a heat transfer effectiveness, defined as a total heat flux ratio of the finned enclosure to the unfinned enclosure ($\epsilon = (\bar{q}_t)_N / (\bar{q}_t)_{N=0}$), versus the Rayleigh number as shown in Figure 11. For KR = 390 with $t = 0.005$, the heat transfer effectiveness of the finned square enclosure is drastically increased with the number of fins at a low Rayleigh number, Ra = 10^3 , as a result of increasing effective thermal conductivity in the enclosure; but the dependence of the effectiveness on N is greatly diminished with increasing Rayleigh number. Furthermore, the heat transfer effectiveness of the enclosure fitted with highly conducting fins is found to be declined drastically with the increase of the Rayleigh number. For instance, an effectiveness of about 46 for N = 4 at Ra = 10^3 in a square finned enclosure decreases down to approximately 4 with Ra increasing up to 10^7 . As for the finned enclosure with KR = 1, the effectiveness, in conformity with the results displayed in Figure 9, is always less than unity and decreases with increasing number of fins, implying that the use of poorly conductive fins in a square enclosure is infeasible for heat-dissipation enhancement.

For the tall enclosures (AR > 1), in contrast to the square enclosure, the presence of the dividing fins of either KR = 1 or

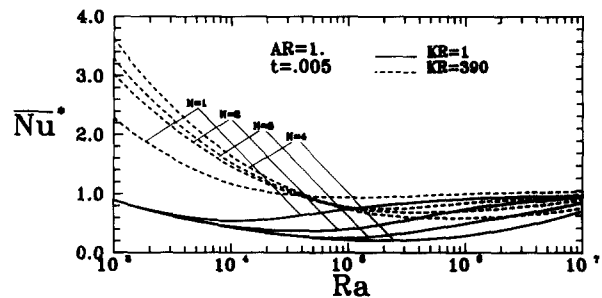


Figure 10 Variation of modified average Nusselt number with Rayleigh number in a square finned enclosure

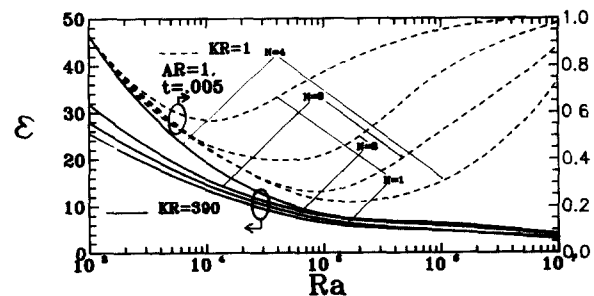


Figure 11 Influence of Rayleigh number on the heat transfer effectiveness in a square finned enclosure

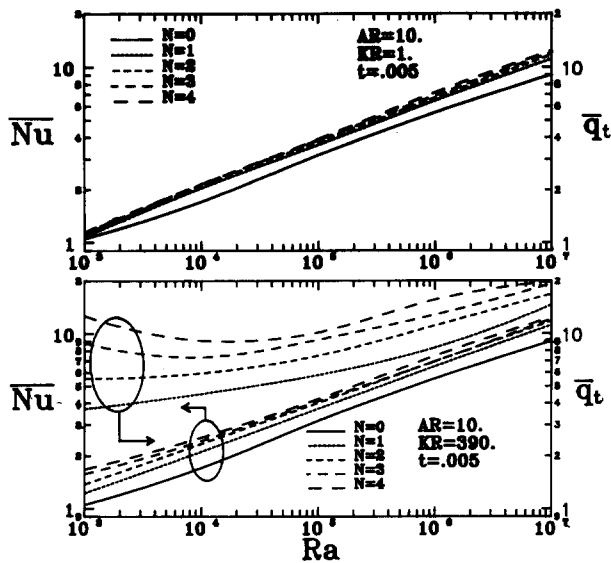


Figure 12 Relation of the average Nusselt number and total heat flux with Rayleigh number in a tall finned enclosure: (a) KR = 1; (b) KR = 390

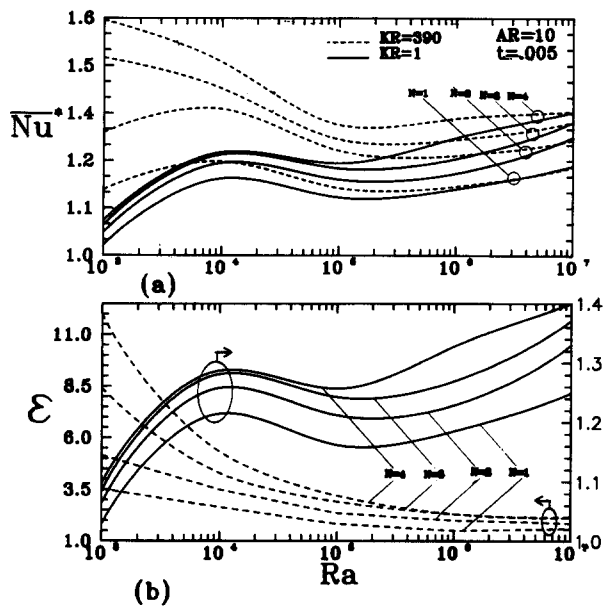


Figure 13 Variations of (a) the modified average Nusselt number and (b) the total heat flux with the Rayleigh number in a tall finned enclosure

KR = 390 may induce marked heat transfer augmentation, as exemplified in Figure 12 for the average Nusselt number as well as for the total heat flux in a finned enclosure of AR = 10. The increase in heat transfer on the fluid-wetted hot wall of the tall finned enclosure, as indicated by the modified average Nusselt number displayed in Figure 13a, becomes further pronounced with the increasing number of fins for both KR = 1 and 390. Moreover, the relation of the modified average Nusselt number with the Rayleigh number in Figure 13a shows significant dependence on the thermal conductivity ratio as well as on the number of fins. The modified average Nusselt number for KR = 1 exhibits a rather nonmonotonic variation with increasing Ra by the occurrence of a local maximum/minimum. A similar trend of \bar{Nu}^* can also be observed for KR = 390 with $N = 1$ and $N = 2$. As for $N = 3$ and $N = 4$ of KR = 390, the

modified average Nusselt number displays a significant drop as Ra is increased from 10^3 to 10^5 , and thereafter shows a slightly rising trend with increasing Ra. Another important observation from Figure 13a is that the influence of KR on the increase in heat transfer from the fluid-wetted surface in the finned tall enclosure becomes minute with increasing Ra, as indicated by the converging of the curves for KR = 1 and 390 at $Ra = 10^7$, both having, for instance, about 40 percent heat transfer enhancement with $N = 4$. As for the effectiveness of the total heat transfer across the finned tall enclosure, presented in Figure 13b for AR = 10 and $t = 0.005$, it can be seen that the effectiveness for KR = 390 is much higher than that for KR = 1. Further, the effectiveness for either case tends to increase with increasing number of fins. Closer inspection of Figure 13b reveals that the effectiveness and the increase of the total heat transfer with increasing number of fins for KR = 390 degrade drastically with increasing Ra. For instance, for $N = 4$ an effectiveness of about 12 at $Ra = 10^3$ drops to about 2.1 at $Ra = 10^7$. On the other hand, the effectiveness for KR = 1 with AR = 10 varies rather nonmonotonically with the increasing Rayleigh number. With Ra increasing from 10^3 to 10^7 , the effectiveness for KR = 1 exhibits a variation of rise and drop-off prior to a monotonic increase trend with Ra. Moreover, in contrast to the observation for KR = 390, the sensitivity of the effectiveness for KR = 1 to the number of fins appears to be further provoked with increasing Ra.

Next, Figure 14 presents the typical influence of the aspect ratio on the heat transfer effectiveness across the finned enclosure with KR = 1, $t = 0.005$ at $Ra = 10^7$. It can be observed from the figure that beyond a certain value of the aspect ratio, the effectiveness for the enclosure fitted with a smaller number of fins can be superseded by that with a larger number of fins so that the effectiveness increases with the number of fins at AR = 10, in contrast to the result indicated in Figure 11 for the square finned enclosure.

The dependence of the heat transfer effectiveness on the dimensionless fin thickness is further illustrated in Figure 15

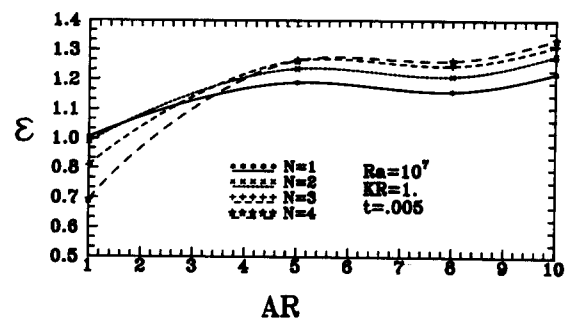


Figure 14 Typical effect of the aspect ratio on the heat transfer effectiveness in finned enclosures

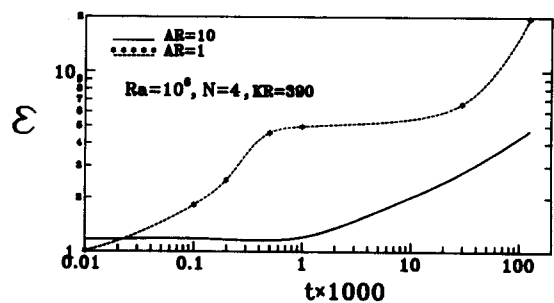


Figure 15 Variation of heat transfer effectiveness in finned enclosures with the dimensionless fin thickness

for $KR = 390$, $N = 4$, and $Ra = 10^6$. For the tall finned enclosure ($AR = 10$), the effectiveness is essentially insensitive to variations of fin thickness for $t < 0.001$, beyond which the effectiveness is greatly enhanced with increasing fin thickness. As for the square finned enclosure, the effectiveness tends to increase sharply as the fin thickness increases, except in the thickness range between 0.0005 and 0.03, where only a moderate increase of the effectiveness is seen.

Finally, using a least squares regression, the heat transfer results for $t = 0.005$ were correlated in the following forms:

$$(\overline{Nu})_N = 0.229 Ra^{0.260}(1 + N)^{0.106} AR^{-0.150} \quad (9a)$$

for $KR = 1$, $Ra = 10^3-10^7$, $AR = 5-10$, and $N = 0-4$, with an average deviation of 3.55 percent;

$$(\overline{Nu})_N = 0.136 Ra^{0.305} N^{-0.245} \quad (9b)$$

for $KR = 390$, $AR = 1$, $Ra = 10^5-10^7$, $N = 1-4$, with an average deviation of 5.7 percent,

$$\bar{q}_t = 8.14 Ra^{0.116} N^{0.214} \quad (9c)$$

for $KR = 390$, $AR = 1$, $Ra = 10^3-10^7$, $N = 1-4$, with an average deviation of 4.45 percent;

$$(\overline{Nu})_N = 0.219 Ra^{0.231}(1 + N)^{0.218} \quad (9d)$$

for $KR = 390$, $AR = 10$, $Ra = 10^3-10^7$, $N = 0-4$, with an average deviation of 2.95 percent; and

$$\bar{q}_t = 1.21 Ra^{0.144} N^{0.392} \quad (9e)$$

for $KR = 390$, $AR = 10$, $Ra = 10^4-10^7$, $N = 1-4$, with an average deviation of 6.4 percent. Little success was obtained in an attempt to develop a global correlation of the heat transfer rate; certainly a further extensive parametric study for the problem is needed in future work.

Concluding remarks

In this study, the effects of conducting horizontal fins on heat transfer due to conjugate natural convection-conduction are investigated numerically for vertical rectangular enclosures. Numerical results are presented for two different values of thermal conductivity of the fin, with water as the working fluid in the divided subenclosures. It is found that for tall enclosures ($AR > 1$), the presence of the dividing horizontal fins, in general, can result in (more or less) heat transfer enhancement for the aspect ratio of the enclosure larger than a certain value, depending on the Rayleigh number as well as the number of fins. As for the square finned enclosure, the use of aluminum fins ($KR = 390$) can lead to considerable heat transfer augmentation, which also depends on the Rayleigh number and the number of fins, while a reduction of heat transfer arises when using the poorly conductive fins ($KR = 1$). Above all, the feasibility and effectiveness of using the dividing horizontal fins to enhance heat transfer across a vertical rectangular enclosure depends strongly on the aspect ratio, the Rayleigh number, the thermal conductivity ratio, and the number of fins.

Acknowledgment

The constructive comments of the reviewers are sincerely appreciated. The computing facility and time required for this study were kindly provided by the computing center of National Cheng Kung University.

References

- Acharya, S. and Jetli R. 1990. Heat transfer due to buoyancy in a partially divided square box. *Int. J. Heat Mass Transfer*, **33**, 931-942
- Acharya, S. and Tsang, C. H. 1985. Natural convection in a fully partitioned, inclined enclosure. *Numer. Heat Transfer*, **8**, 406-428
- Bajorek, S. M. and Lloyd, J. R. 1982. Experimental investigation of natural convection in partitioned enclosures. *J. Heat Transfer*, **104**, 527-532.
- Bejan, A. 1984. *Convective Heat Transfer*. John Wiley and Sons, New York
- de Vahl Davis, G. 1983. Natural convection of air in a square cavity: a benchmark solution. *Int. J. Numer. Methods Fluids*, **3**, 249-264
- Fletcher, C. A. J. 1988. *Computational Techniques for Fluid Dynamics I*. Springer-Verlag, New York
- Frederick, R. L. 1989. Natural convection in an inclined square enclosure with a partition attached to its cold wall. *Int. J. Heat Mass Transfer*, **32**, 87-94
- Ho, C. J. and Jeng, J. D. 1989. A holographic interferometry study of natural convection in a fully-partioned air-filled enclosure. *J. Chinese Inst. Engineers*, **12**, 101-107
- Ho, C. J. and Yih, Y. L. 1987. Conjugate natural convection heat transfer in an air-filled rectangular cavity. *Int. Comm. Heat Mass Transfer*, **14**, 91-100
- Kangni, A., Ben Yedder, R., and Bilgen, E. 1991. Natural convection and conduction in enclosures with multiple vertical partitions. *Int. J. Heat Mass Transfer*, **34**(11), 2819-2825
- Leonard, B. P. 1983. A convectively stable, third-order accurate finite difference method for steady two-dimensional flow and heat transfer. In *Numerical Properties and Methodologies in Heat Transfer*, Shih, T. M. (ed.). Hemisphere, Washington, DC, 211-226
- Lin, N. N. and Bejan, A. 1983. Natural convection in a partially divided enclosure. *Int. J. Heat Mass Transfer*, **26**, 1867-1878
- Mishimura, M., Shiraishi, M., Nagasawa, F., and Kawamura, Y. 1988. Natural convection heat transfer in enclosures with multiple vertical partitions. *Int. J. Heat Mass Transfer*, **31**, 1679-1686
- Nansteel, M. W. and Greif, R. 1981. Natural convection in divided and partially divided rectangular enclosures. *J. Heat Transfer*, **103**, 623-629
- Oosthuizen, P. H. and Paul, J. T. 1985. Free convection heat transfer in a cavity fitted with a horizontal plate on the cold wall. In *Advance in Enhanced Heat Transfer-1985*, Shenkman, S. M., et al. (eds.), vol. 43. ASME HTD, New York
- Ostrach, S. 1988. Natural convection in enclosures. *J. Heat Transfer*, **110**, 1175-1190
- Ramman, N. and Korpela, S. A. 1989. Multigrid solution of natural convection in vertical slot. *Numer. Heat Transfer*, part A, **15**, 323-339
- Saitoh, T. and Hirose, K. 1989. High-accuracy benchmark solutions to natural convection in a square cavity. *Computational Mech.*, **4**, 417-427
- Shakerin, S., Bohn, M., and Loehrke, R. I. 1986. Natural convection in an enclosure with discrete roughness element on a vertical heated wall. *Heat Transfer-1986*, **4**, 1519-1525
- Tong, T. W. and Gerner, F. M. 1986. Natural convection in partitioned air-filled rectangular enclosure. *Int. Comm. Heat Mass Transfer*, **13**, 99-108